Climate-modulated nutrient conditions along the Labrador Shelf: Evidence from nitrogen isotopes in a six-hundred-year-old crustose coralline alga

John M. Doherty[1], Branwen Williams[2], Esme Kline[2], Walter Adey[3], & Benoit Thibodeau[1]

[1]Department of Earth Sciences & Swire Institute of Marine Science, The University of Hong Kong, Pokfulam Rd., Hong Kong SAR

[2]W.M. Keck Science Department, Claremont McKenna College, Pitzer College, Claremont, CA, USA

[3]Department of Botany, Smithsonian Institution, Washington DC, USA

Correspondence:

Branwen Williams (bwilliams@kecksci.claremont.edu)

Benoit Thibodeau (bthib@hku.hk)

Abstract

The impacts of climate change on North Atlantic nutrient chemistry remain poorly understood, as there exist a multitude of rapidly-changing biological and physical drivers of nutrient conditions throughout the region. Here, we present nitrogen isotope measurements derived from a six-hundred-year-old crustose coralline alga ($\delta^{15}N_{algal}$) to elucidate historic and contemporary trends in Labrador Shelf nitrate utilization, defined as the degree of biological nitrate uptake relative to supply. Prior to ~1800, periods during which utilization approached completion corresponded to neutral modes of the Atlantic Multidecadal Oscillation, which we argue promoted favorable oceanographic conditions for simultaneous phytoplankton growth and reduced nitrate input. More recently, nearly-complete utilization occurred concomitantly with a weakened Labrador Current, suggesting reduced nutrient inflow from eastern subpolar waters. These results highlight the role of ongoing climate-induced circulation changes in driving nutrient distributions throughout the subpolar North Atlantic, which may have implications for future fisheries and oceanic carbon storage.

1 Introduction

High-latitude regions suffer the greatest impacts of modern-day climate change (*1*). One effect of this change is enhanced sea-ice melt along the Labrador Shelf (*2*), which is driving an unprecedented increase in primary productivity relative to the past several hundred years (*3*). While such a dramatic change in productivity should intuitively lead to the greater depletion of upper-ocean nutrients, multiple simultaneous environmental changes throughout the region make this relationship less straightforward. This is because nutrient availability in the subpolar North Atlantic is not only a function of biological activity, but also of physical oceanographic processes that regulate nutrient supply.

The Labrador Sea in the north Atlantic Ocean receives considerable scientific attention because deep-water convection in the region is thought to be historically important for driving the strength of the Atlantic meridional overturning circulation (AMOC) (*4*, *5*). Paleoceanographic investigations suggest that convection in the Labrador Sea has been at an anomalously weak state over the last ~150 years, most likely due to anthropogenic warming and freshwater forcing (*6*–*8*). Recent observations further suggest that convection in the Labrador Sea has been virtually shut off (*9*), which has weakened the Labrador Current and resulted in its retreat away from the north-western Atlantic coast (*6*). Because this current transports nitrate-rich waters derived from the eastern subpolar region to the Labrador Shelf (*10*), such a reorganization of upper-ocean circulation patterns may have implications for primary productivity, regionally-important fisheries (*11*) and oceanic carbon storage (*12*). Due to the absence of long-term observational data, however, paleo-proxies are required to contextualize these contemporary changes and their effects on nitrate delivery.

Along the coastal Labrador Shelf, nitrate is supplied during winter via vertical mixing (*13–15*) and advection from the eastern subpolar region (*10*). Advective supply relies on the Labrador Current, which sources waters from the eastern region of the subpolar Atlantic, Baffin Bay and Hudson Strait (Figure 1). Eastern subpolar waters are comprised of Arctic outflow, sourced from the East Greenland Current, and Atlantic inflow, sourced from the North Atlantic Current, an extension of the Gulf Stream. At the central shelf, nitrate is likely predominately derived from the eastern region, as concentrations north of the shelf are negligible relative to those observed at mid-shelf latitudes (Figure 1). Moreover, previous field surveys indicate that nutrient outflow from the Hudson Strait only impacts the northern-most tip of the shelf (*16*), which suggests that northern-sourced nitrate is mostly restricted from entering the mid-shelf region. While terrestrial input may constitute an additional nitrate source, annual runoff is only 600 – 700 mm along the coast (*17*). Such a source would be diluted by the Labrador Current, which travels at a velocity of 0.8 Sv (*18*). As such, nitrate supply along the mid-shelf region is primarily affected by vertical mixing and advection, which today is mostly completely consumed during the phytoplankton growing season (Figure 1). The degree of nitrate consumption relative to supply, known as utilization (*19*), imprints an isotopic fingerprint on biologically-assimilated nitrogen due to kinetic fractionation processes that result in the preferential assimilation of ^{14}N-nitrate in photosynthetic organisms (*20*). Under conditions of low utilization, preferential assimilation of the light isotope results in biologically-assimilated nitrogen depleted in the heavy isotope. As utilization approaches completion, isotopic discrimination becomes less common and the isotopic composition of biologically-assimilated nitrogen approaches that of the initial nitrate source (*20*). This utilization-induced nitrogen

fractionation appears to be a universal feature among all marine photosynthetic organisms that have been studied (*21*), including macro-benthic algae (*22*).

Nitrogen is preserved in a variety of geologically-important marine organisms, such as foraminifera (*23*), corals (*24*) and bivalves (*25*). Over the last few decades, crustose coralline algae have also emerged as promising paleoenvironmental archives due to their widespread distribution, significant longevity and annual banding patterns, the latter of which allows for precise and high-resolution reconstructions of oceanographic changes in the recent geological past (*2*, *3*, *26*, *27*). As such, the $\delta^{15}N$ of nitrogen retained in the organic matter of coralline algae may offer a unique window into the history of marine nutrient dynamics on multicentennial timescales. Here, we present a ~5-year-resolved $\delta^{15}N$ record derived from a 613-year-old crustose coralline alga, *Clathromorphum compactum* ($\delta^{15}N_{algal}$), and demonstrate its utility in reconstructing coastal variability along the rapidly-changing Labrador Shelf throughout the last several centuries (Figure 2). Because a variety of factors may impact the isotopic composition of biologically-assimilated nitrogen, we compare our record with several other high-resolution paleoenvironmental reconstructions to infer the most likely drivers of $\delta^{15}N_{algal}$ variations over the last several hundred years.

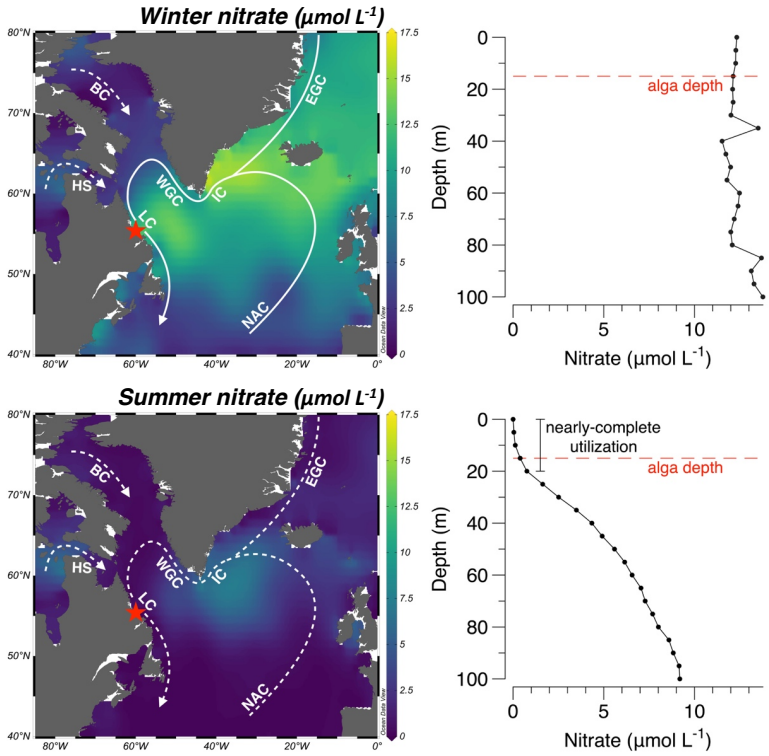

Figure 1: Seasonal oceanography and modern nitrate conditions. (left) Surface maps of **(top)** winter and **(bottom)** summer nitrate distributions and the major surface currents involved in the supply of nitrate to the study site, indicated by the red star. Solid-lined currents indicate upper-ocean pathways that are strongly involved in the seasonal supply of nitrate to the study site and dashed-lined currents represent a weak seasonal involvement in nitrate supply. Abbreviations: NAC: North Atlantic Current, IC: Irminger Current, EGC: East Greenland Current, WGC: West Greenland Current, LC: Labrador Current, BC: Baffin Current, HS: Hudson Strait outflow. **(right)** Depth profiles of **(top)** winter and **(bottom)** summer nitrate concentrations at 55.5 °N, 58.5 °W. This figure was generated with the help of Ocean Data View (*28*) using inorganic nutrient data taken from the World Ocean Atlas (*29*).

2 Results and discussion

2.1 Regional biogeochemical and climatic influences on nitrogen isotope fractionation

Our record spanned from 1392 to 2005. During this period, $\delta^{15}N_{algal}$ values generally followed an increasing trend from -0.3 to 7.9‰ (Figure 2). $\delta^{15}N_{algal}$ initially increased by ~7‰ from 1392 to

the late 1500s prior to a transition to relatively constant average values, during which there were 4 notable periods characterized by values typically between 6 and 7‰ spaced by approximately 100 years. In 1871, $\delta^{15}N_{algal}$ increased by an average of ~2.9‰, with high values persisting throughout the remainder of the study period.

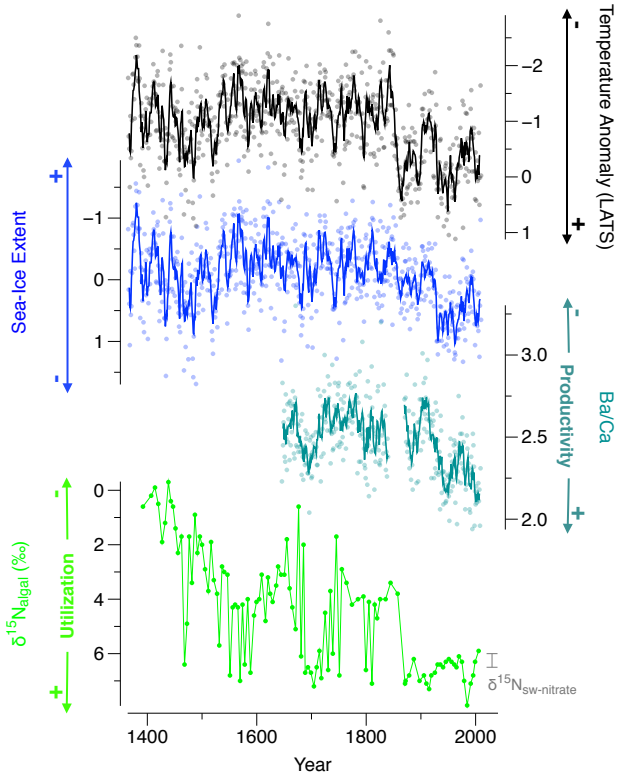

Figure 2: Environmental changes in the Labrador Shelf archived in coralline algae. (top to bottom) Temperature reconstructed from the Labrador Algae Time Series (LATS) reported in (*27*)), significantly correlated with observational temperature data (Table S1); historical algal-derived inverse index of regional sea-ice extent (*2*); algal Ba/Ca ([(µg g^{-1})/(µg g^{-1}) × 10^{-5}]), inversely representative of productivity (*3*); and nitrate utilization reconstructed via the isotopic composition of algal nitrogen. Lines for temperature anomalies, sea-ice extent and Ba/Ca represent five-year-smoothed means of the data. Contemporary isotopic signature of dissolved nitrate in the Labrador Current (*30*) and throughout the eastern subpolar region (*31*) is represented by the grey bars on the bottom panel.

$\delta^{15}N_{algal}$ values reflect the isotopic signature of ambient nitrogen (*22*), which may be controlled by the original isotopic signature of the local nitrogenous nutrient pool and its fractionation by biological and biochemical processes. In the Labrador Sea, this is likely governed by the isotopic composition and fractionation of seawater nitrate, as other species of nitrogen, such as ammonium, are considered unimportant for primary productivity along the Labrador Shelf and throughout the larger Labrador Sea region (*14*). Isotopic variations driven by chemical transformations of seawater nitrate, such as input reactions (i.e., atmospheric dinitrogen fixation) and removal reactions (i.e., reduction via denitrification), would impart isotopically lighter and heavier signals on the $\delta^{15}N$ of seawater nitrate, respectively. However, *in-situ* denitrification is likely implausible, as high ambient oxygen concentrations (~8 mL L^{-1}) exist along the Labrador Shelf (*32*), whereas near-zero oxygen concentrations are required to favor such an anaerobic metabolism (*33*). It is conceivable that denitrification occurring in the north Pacific could affect the baseline isotopic composition of nitrate feeding the Baffin Bay and thus the north-western source waters of the Labrador Current. Yet, even during the winter productivity minima, nitrate concentrations are relatively much lower in Baffin Bay compared to our study site (Figure 1), suggesting a negligible nitrate supply from Pacific sources to the polar North Atlantic. Additionally, because outflow from the Hudson Strait is nearly completely consumed at the northern tip of the shelf (*16*), the minimal nitrate derived from north-western source waters would be assimilated at higher latitudes prior to its arrival to the mid-shelf. As such, biogeochemical dynamics in the north Pacific cannot plausibly explain isotopic variations at the central Labrador Shelf.

Arctic cyanobacteria fix atmospheric dinitrogen at similar rates to their low-latitude counterparts, which suggests that fixation may play an important role in high-latitude nitrogen cycling (*34*). Arctic fixation could lower the isotopic composition of seawater nitrate, feed into the East Greenland Current and eventually reach the Labrador Shelf (Figure 1). However, fixation should be positively related to temperature due to the requirement of open-ocean conditions for both cyanobacterial growth and Arctic throughflow (*35*), and so the lack of a clear relationship between elevated temperatures and lower $\delta^{15}N_{algal}$ throughout the record argues against such a mechanism. In fact, the last ~130 years in our record reflect simultaneously the warmest conditions and the highest $\delta^{15}N_{algal}$ values (Figure 2). As such, dinitrogen fixation is not a likely control on $\delta^{15}N_{algal}$, leaving nitrate utilization as the last remaining plausible driver of the record.

Nitrate utilization as the driving mechanism of $\delta^{15}N_{algal}$ is supported by the most recent measurements in our record, which approximate the $\delta^{15}N$ of nitrate throughout the upper waters (100 m) of the Labrador Sea (~6 – 6.5‰, Figure 2) (*30*), as would be expected during the nearly-complete consumption (*22*) characteristic of the contemporary period (Figures 1 and 2). Additionally, similar $\delta^{15}N$ signatures of seawater nitrate are reported in surface waters of the eastern subpolar region (*31*), which suggests an isotopically-homogenous nitrate flow throughout the upper-ocean subpolar Atlantic. Interestingly, during each period of high $\delta^{15}N_{algal}$, the isotopic signature also approximates this range (Figure 2), which would be coherent with phases of nearly-complete nitrate utilization (*19*) (Figure 2). Nearly-complete utilization may be caused by increased biological uptake, reduction of nitrate supply or a combination of both. Over the last century, productivity reconstructed from algal Ba/Ca (*3*) has been highly variable while $\delta^{15}N_{algal}$ values remained relatively constant (Figure 2). This implies that nitrate utilization during this

interval was at least partially controlled by changes in nitrate supply, rather than exclusively by changes in biological uptake.

Although nitrate is supplied during winter, its vertical fluxes may be further affected by the degree of upper-ocean stratification during summer, which sets the limit of nitrate mixed to the photic zone available for biological uptake (*13–15*). Upper-ocean stratification is driven by both temperature and salinity, which are positively correlated along the Labrador Shelf (*36*) (Table S1). This suggests that cold and fresh meltwater significantly impacts regional upper-ocean temperatures such that anomalously high stratification forced by large inputs of freshwater should also correspond to anomalously negative temperature excursions. Alternatively, anomalously high stratification forced by upper-ocean warming should correspond to anomalously positive temperature excursions. However, there is no indication of anomalous, empirically-validated (Table S1) paleo-temperature reconstructions based on growth-normalized Mg/Ca in the algal specimen, i.e. the "LATS" (*27*), reflecting high stratification during phases of nearly-complete nitrate utilization, as the average magnitudes of temperature anomalies during these time periods are either below or close to average pre-1850 values (Figure 3). While it is true that temperature anomalies along the Labrador Shelf were generally more positive beginning at the onset of the most recent phase, they also exhibited high variability. Such variability is not reflected in $\delta^{15}N_{algal}$ values, which remained persistently enriched in the heavy isotope since ~1870 (Figure 2). In other words, upper-ocean stratification via excessive freshwater forcing or excessive upper-ocean warming cannot likely explain the existence of phases of nearly-complete utilization. This suggests that advective supply from the Labrador Current played a key role in regulating past nitrate conditions along the Labrador Shelf.

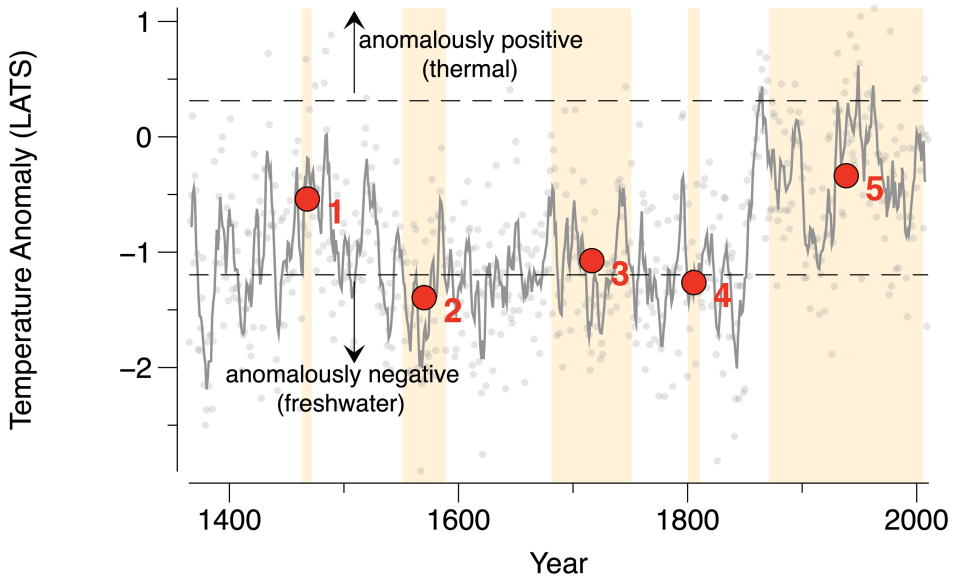

Figure 3. Temperature anomalies as a proxy for upper-ocean stratification. Average positive and negative pre-1850 temperature (LATS) anomalies (*27*) are represented by the horizontal dashed lines and average temperature (LATS) anomalies during each phase of nearly-complete nitrate utilization are represented by the red dots. Values that exceed the pre-1850 mean value in either sign are considered to correspond to high stratification via thermal forcing (positive) in the case of the former and freshwater forcing (negative).

Because changes in the trajectory of the Labrador Current are associated with changes in regional deep-water formation, the historical variability of regional convection may help to inform past variations in the current's coastal flow and its impact on nitrate supply. Deep-water formation is typically discussed in terms of its relationship with broader climatic fluctuations; notably, the North Atlantic Oscillation (NAO) and Atlantic Multidecadal Oscillation (AMO), which are intimately connected to temperature and circulation patterns in the North Atlantic. While recent work indicates that the AMO may not be an oscillation per se, and may be more appropriately termed "Atlantic multidecadal variability" (*37*), here we use the original AMO language to be consistent with previous authors that have generated paleo-reconstructions of its behavior.

The NAO describes the atmospheric pressure gradient between the Icelandic Low and Azores High systems, which is conventionally expressed by an index that assigns positive values (NAO+) to increased pressure differences and negative values (NAO-) to decreased pressure differences (*38*). Relevant to our work, previous hydrographic investigations suggest that NAO- conditions facilitate enhanced advection of Labrador Current waters to the coastal shelf (*39*). The AMO describes multidecadal sea-surface temperature (SST) variations characteristic of the North Atlantic basin. Like the NAO, it is typically discussed in terms of an index, where positive index values (AMO+) represent multidecadal-scale positive SST anomalies and negative index values (AMO-) represent multidecadal-scale negative SST anomalies (*40*). In the Labrador Sea, the AMO- mode is associated with increased cooling and sea-ice extent (*41*) along with decreased productivity (*3*), while the AMO+ condition is characterized by the opposite. A recent synthesis of observational data, modeling studies and paleoclimate reconstructions suggests that the AMOC is responsible for driving this multidecadal variability throughout the Atlantic, with AMO+ conditions corresponding to a strong AMOC and AMO- conditions corresponding to a weak AMOC (*42*). Numerical simulations additionally demonstrate that this variability has been significantly associated with the strength of the AMOC on 100-year periodicities throughout the last 1400 years (*43*), reminiscent of the approximate pacing of nearly-complete nitrate utilization phases present in our record. Below, we illustrate the relevance of the NAO and AMO in modulating nitrate conditions along the Labrador Shelf, and how weakening of the Labrador Current beginning around 1800 has disrupted these historical dynamics.

2.2 Pre-1800 drivers: Primary productivity and nitrate supply

249 The five phases of nearly-complete nitrate utilization interpreted from high $\delta^{15}N_{algal}$ values over
250 the last 600 years may either be driven by increases in primary productivity or decreases in nitrate
251 supply. Because the extent of sea-ice demise is the main driver of productivity along the Labrador
252 Shelf (*3*), and because direct productivity reconstructions are not available until after 1600, we
253 infer indirect productivity changes from paleo-reconstructed sea-ice cover for earlier time intervals
254 in our record (*2*). Coherence of decreased sea-ice extent (and thus, inferred increased productivity)
255 with increased $\delta^{15}N_{algal}$ values until 1500 supports a productivity-driven change in nitrate
256 utilization (Figure 4a). However, $\delta^{15}N_{algal}$ leads sea-ice index values, suggesting that productivity
257 could not have controlled nitrate utilization during this brief first phase of nearly-complete
258 utilization (~1470). Furthermore, a significant antiphase association between the sea-ice index and
259 $\delta^{15}N_{algal}$ during phase 2 (~1550 – 1590) indicates that increased sea-ice extent (and thus, inferred
260 decreased productivity) occurred in tangent with increased $\delta^{15}N_{algal}$ values. Because decreased
261 productivity should normally result in lower nitrate utilization, and thus lower $\delta^{15}N_{algal}$ values, such
262 a relationship discredits productivity as the main driver of nitrate utilization during this interval.
263 In the 1600s, reconstructions of productivity become available from algal Ba/Ca data (*3*). The
264 onset of phase 3 (~1680 – 1720; hereafter, 3_1) occurred in concert with an increase in productivity
265 reconstructed from algal Ba/Ca (Figure S1). However, edge effects characteristic of the wavelet
266 analysis between Ba/Ca and $\delta^{15}N_{algal}$ prevent a robust statistical comparison of these variables
267 during this period (Figure S1), and sea-extent reconstructions do not support a significant
268 relationship between productivity and $\delta^{15}N_{algal}$ (Figure 4a). Moreover, elevated $\delta^{15}N_{algal}$ values
269 were maintained well after phase 3_1, until ~1750, corresponding to low Ba/Ca-reconstructed
270 productivity (Figure S1); thus, nitrate supply was likely important for driving the first three phases.
271

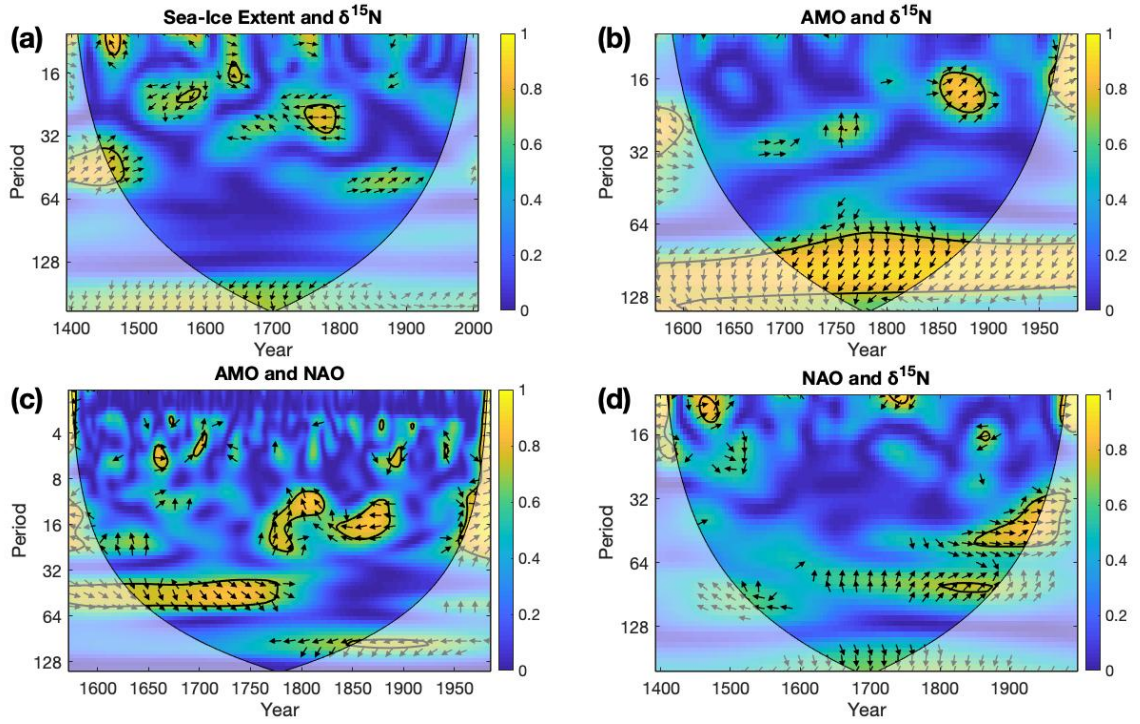

Figure 4: Cross-wavelet coherence and phase relationships between (a) sea-ice extent and $\delta^{15}N_{algal}$, (b) AMO and $\delta^{15}N_{algal}$, (c) AMO and NAO and (d) NAO and $\delta^{15}N_{algal}$. Significant overlaps in spectral power between signals at the 95% confidence level against red noise are represented within the black contours. Arrows indicate phase relationships, where leftward-pointing represents an antiphase relationship, rightward-pointing represents an in-phase relationship, downward-pointing represents the first series (written on the left side of the title) leading the second series and upward-pointing represents the opposite. The areas in which edge effects may interfere with analyses are depicted by the shaded regions. All analyses were performed in MatLab R2019a using default options in the Cross Wavelet and Wavelet Coherence toolbox provided by A. Grinsted. For specifications of the relevant calculations, the reader is referred to the original publication (*44*).

With the exception of phase 3_1, phases of nearly-complete nitrate utilization prior to 1800, corresponded to relatively neutral AMO and NAO modes reconstructed from tree and speleothem archives (*45*, *46*) (Figure 5a and 5b), with the AMO persistently significantly influencing nitrate utilization on periodicities of approximately 100 years (Figure 4b). The AMO led the NAO in a significant, in-phase association throughout this time frame (4c), although no effect of the NAO

on utilization is recorded (4d). Because the AMO is associated with upper-ocean circulation patterns (*42*), these results suggest that ocean circulation played a dominant role in driving utilization and the NAO until the late 1700s. Neutral-mode AMO conditions may support a favorable oceanographic setting for a simultaneous reduction in advective nitrate supply while maintaining a sufficient level of primary productivity. Specifically, while a positive-mode AMO is associated with sea-ice reductions in the Labrador Sea and therefore drives increases in productivity (*3*) and nitrate uptake, such a condition also corresponds to strong AMOC conditions (*42*), and thus a strong Labrador Current, responsible for supplying nitrate to the region. Conversely, a negative-mode AMO corresponds to sea-ice expansion and therefore favors lowers productivity, but its reliance upon a weak Labrador Current may result in reduced nitrate supply. Thus, the effects of high-amplitude variations in the AMO on nitrate utilization could be subdued due to the nature of both extremes producing simultaneously equal effects on both productivity and nitrate supply (Figure 6). As such, we suggest that nitrate utilization was maximized during "Goldilocks" conditions corresponding to relatively neutral AMO forcing, also driving neutral NAO forcing, characteristic of phases 2 and 3 (Figure 5b). While AMO reconstructions do not extend to the time period of phase 1, neutral-type NAO conditions also persist throughout this interval (Figure 5a). If the relationship between the AMO and NAO during phase 1 was similar to that observed during phases 2 and 3, this may indicate a similar "Goldilocks" mechanism at play.

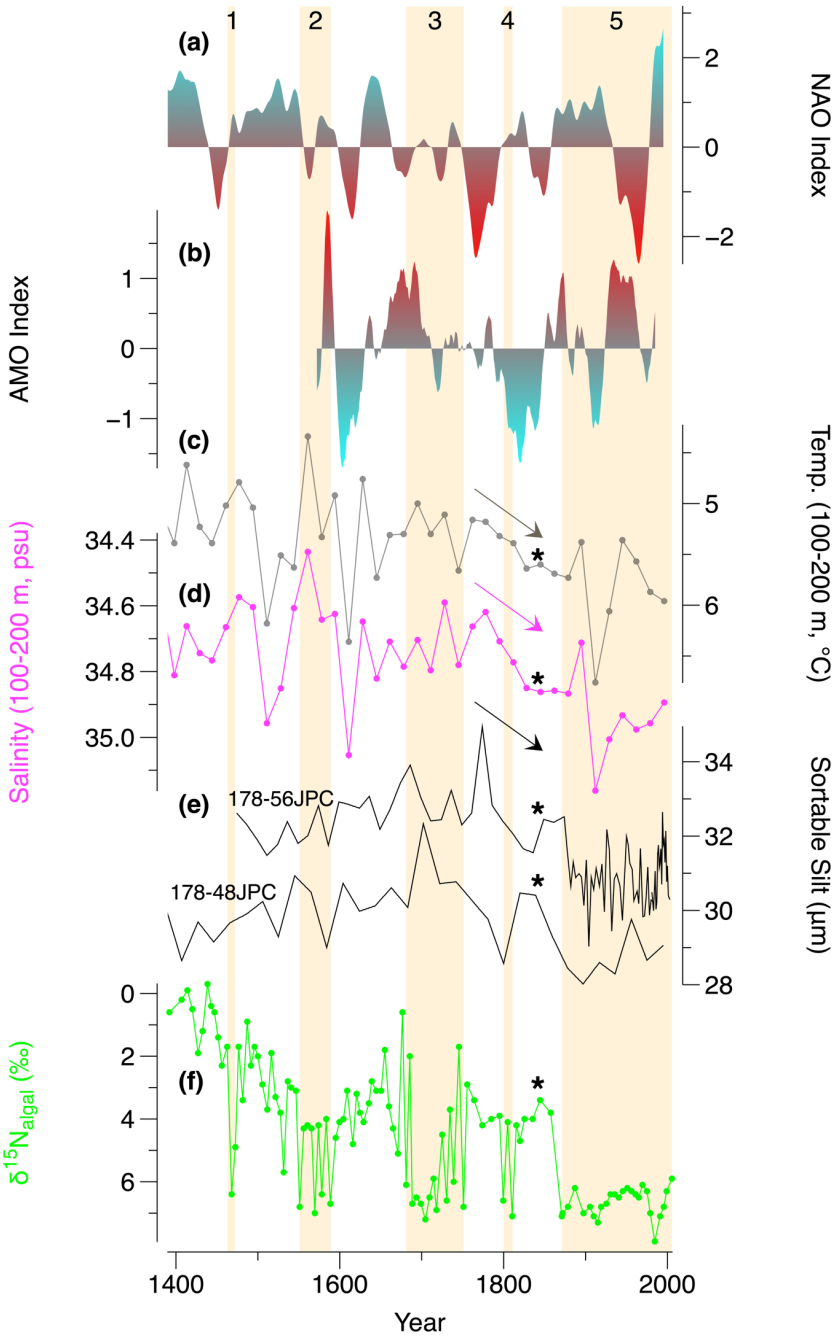

Figure 5: Ocean-atmosphere processes and their effects on the Labrador Sea. (a) NAO index reconstructed from tree and speleothem archives (*45*); **(b)** AMO index reconstructed from tree-ring analysis (*46*); Labrador Sea convection reconstructed from **(c)** temperature and **(d)** salinity at 100 – 200 m depth (*47*), and from **(e)** mean sortable silt (*7*); and **(f)** nitrate utilization. In NAO and AMO plots, colors correspond to cold (blue) and warm (red) conditions associated with each mode in the Labrador Sea region. The vertical shaded regions correspond to phases of nearly-complete nitrate utilization. Arrows denote the initial weakening of Labrador Sea convection and asterisks denote the potential pause or reversal of convection weakening.

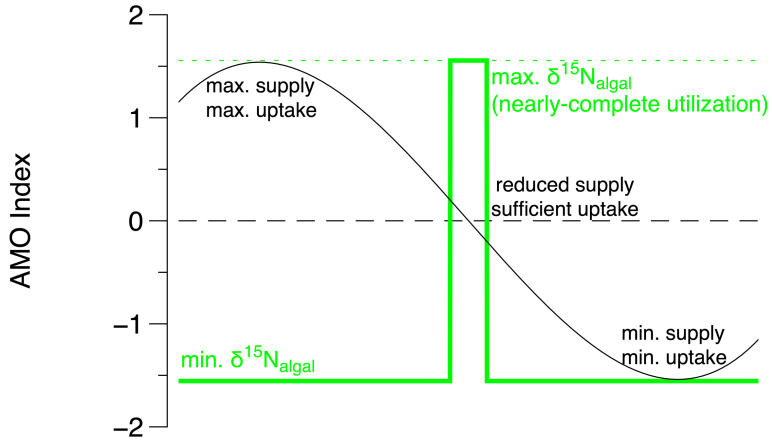

Figure 6: Schematic model of the historic "Goldilocks" nitrate utilization mechanism. Utilization (green) is maximized to near completion coincident with neutral AMO (black) conditions, which are hypothesized to reduce advective nitrate supply while simultaneously allowing for sufficient phytoplankton growth and biological uptake.

2.3 Post-1800 drivers: Reductions in advective supply

In the late 1700s, the relationship between the NAO and AMO changed. A transient, higher-frequency interval of significance is recorded between the two parameters, but variable phase relationships characteristic of this association argue against it being mechanistically important (*44*) (Figure 4c). During the onset of phase 4, ~1800, the AMO was at its most pronounced and long-lived negative mode, which corresponded to a weakening of Labrador Sea convection inferred from salinity and temperature reconstructions at 100 – 200 m depth (*47*) (Figure 5c and 5d) and from mean sortable silt records (*7*) (Figure 5e). Because convection in the Labrador Sea affects the trajectory of the Labrador Current, such a weakening may have resulted in reduced inflow of eastern-derived nitrate-rich waters to the shelf during this interval.

Phase 4 (~1800 – 1810) was initiated during a period of low productivity, as shown by the significant antiphase association between the sea-ice index and $\delta^{15}N_{algal}$ near the onset of the brief interval (Figure 4a). Further, significant relationships between Ba/Ca and $\delta^{15}N_{algal}$ occurred in-phase during this interval. Since the Ba/Ca proxy is inversely related to productivity, this indicates that periods of low productivity corresponded to periods of high nitrate utilization. As such, productivity cannot explain the occurrence of phase 4. However, this period is characterized by the onset of a statistically significant antiphase association between the AMO and NAO, which is the opposite of that observed during the pre-1800 interval (Figure 4c). Further dissimilar, the AMO stopped leading the NAO during the mid-19th century (Figure 4c), which indicates that a reorganization of ocean-atmosphere dynamics could have occurred during a brief resumption of Labrador Sea convection observed directly after phase 4. Thus, we propose the following scenario to explain nutrient dynamics from ~1800 – 1870: first, nearly-complete utilization from ~1800 – 1810 was driven by a decreased supply of nitrate forced by weaker Labrador Current inflow. The decrease in nitrate utilization following phase 4 was then caused by the resumption of nitrate supply driven by a reinvigorated Labrador Sea convection (*7*, *47*) and coastal Labrador Current inflow (Figure 5c – f). Such an increase in coastal inflow may be associated with the prevailing negative-mode NAO conditions (Figure 5a), which have been previously shown to facilitate the enhanced advection of Labrador Current waters to the shelf (*39*). This mechanism is supported by the significant in-phase correlations between the NAO and $\delta^{15}N_{algal}$ that emerge during the mid-19th century, suggesting an increased nitrate supply under such an atmospheric configuration (Figures 4d, 5a and 5f). Finally, as NAO conditions shifted in sign, the current once again weakened and limited nitrate supply in the late 1800s, coinciding with the start of phase 5 (Figures 4d, 5a and 5f). However, high-amplitude variability in NAO conditions following the 20th century

369 occurring concomitantly with consistently-elevated $\delta^{15}N_{algal}$ values argue against atmospheric
370 circulation driving nitrate utilization in recent years.
371
372 The onset of the industrial era coincided with dramatic alterations in Labrador Sea oceanography.
373 Over the last 150 years, the Labrador Sea region experienced notable changes in sea-ice extent (*2*),
374 productivity (*3*), circulation strength (*6*, *7*) and nitrate utilization (Figures 2 and 5). Interestingly,
375 nitrate utilization approached completion during this entire interval, making phase 5 (~1870 –
376 present) the longest in our record. However, sea-ice extent and productivity exhibited considerable
377 variability throughout phase 5 (Figure 2). In fact, nitrate utilization was entirely uncorrelated with
378 both sea-ice extent (Figure 4a) and Ba/Ca-reconstructed productivity (Figure S1) throughout the
379 interval, which suggests that biological uptake was unimportant for driving utilization. During
380 phase 5, the AMOC underwent an intense weakening (*8*, *48*), very likely driven by anthropogenic
381 climate forcing, concomitant with strong reductions in Labrador Sea convection (*7*) (Figure 5c –
382 e) and a migration of the Labrador Current away from the coast (*6*). As such, the recent shift in the
383 Labrador Current's trajectory likely reduced advective nitrate supply to the shelf, and is the most
384 plausible mechanism for the anomalously-prolonged phase of nearly-complete utilization
385 characteristic of the last 150 years. This finding supports the previously-proposed hypothesis that
386 biogeochemical changes along the coastal north-western Atlantic may be associated with the
387 larger-scale AMOC decline characteristic of the post-industrial era (*49*).
388
389 **2.4 Environmental implications**
390 While previous studies have commented on the relationships between AMOC strength, nutrient
391 supply and productivity in the North Atlantic, such studies have invoked upper-ocean stratification

as the main mechanism responsible for these associations (*50*, *51*). However, our data suggest that stratification did not play a prominent role in driving nitrate supply to the Labrador Shelf during past and present phases of nearly-complete utilization (Figure 3), and rather highlight the importance of upper-ocean circulation in routing nitrate away from the coast. The ecological and biogeochemical consequences of such nitrate reorganizations in the North Atlantic are not fully understood and should be subject to further research. For example, changing nitrate distributions may alter the locations and extent of primary productivity, which ecological models suggest strongly affects the vulnerable and socioeconomically-important Atlantic cod (*52*). In addition to the possible impacts on regional fisheries, changes in primary productivity may have implications for the future potential of oceanic carbon storage in the region (*12*). Thus, numerous environmental challenges may be exacerbated by anthropogenic disturbances to the North Atlantic.

3 Conclusions

Here, we have described mechanisms related to ocean-climate interactions that drove changes in nutrient dynamics along the Labrador Shelf over the last 600 years. We show that productivity alone cannot explain phases of nearly-complete nitrate utilization in the region, and rather suggest that neutral AMO forcing in the past promoted a "Goldilocks" state during which sufficient biological uptake coupled with changes in nitrate supply allowed for such phases to occur on approximately centennial timescales. Additionally, we demonstrate that the reduction in the strength of the AMOC via its weakening of the Labrador Current likely contributed to a persistently-low supply of nitrate to the Labrador Shelf, resulting in an anomalously-prolonged phase of nearly-complete utilization since ~1870. In contrast to past cycles of nitrate supply and uptake observed along the shelf, nutrient conditions will likely not recover due to the ongoing

retreat of the Labrador Current. Our study thus adds to the abundant body of evidence illustrating the intense sensitivity of the high-latitude North Atlantic region to modern warming.

4 Materials and Methods

4.1 Specimen collection and age model development

A living *C. compactum* specimen was collected off the coast of Kingitok Island, Labrador, Canada (55.3983 °N; 59.8467 °W) at 15 m depth in 2011 via divers using SCUBA (Figure 1). Following collection, the specimen was rinsed in freshwater and cross-sectioned perpendicular to the direction of growth. The cross-section was mounted on a plate using wax and polished with Allied High Tech diamond lapping film and water (30, 15, and 1 μm grains) until growth bands were clearly visible. Using high-resolution images of the specimen taken with a Nikon H600L Microscope, bands were identified and assigned years to develop a growth chronology in Photoshop. Previous U-Th dating indicated that the age of the specimen was ~630 years old (*2*), which was also verified by the number of growth bands counted.

4.2 Isotopic analysis

A high-precision, computer-driven New Wave Research Micromill Sampling System attached to an x, y, and z stage was used to collect (mill) material from along the growth bands for $\delta^{15}N$ analysis. To remove external particulates before drilling, the specimen was sonicated 3 times for 5 minutes in Milli-Q water and then oven-dried for 24 hours. Following the visible growth bands as much as possible, digitized drill paths were programmed on the Micromill screen. For each drill line, 5 to 6 150-μm-deep drill passes were made. The majority of samples were taken at 5-year increments with an average resolution of 3 to 6 years, except for regions of the skeleton where

insufficient material required milling from more growth bands, increasing the resolution to between 7 and 20 years. Each sample consisted of 7 mg of organic-rich material. Following sample collection, pressurized air was used to remove residual sample powder. Samples were weighed in tin cups to obtain the same amount of N_2 for all samples and reference materials. Then, the samples were analyzed using a Micromass Isoprime 100 isotope ratio mass spectrometer coupled to an Elementar Vario MicroCube elemental analyzer operated in continuous-flow mode at GEOTOP (Université du Québec à Montréal). Two internal reference materials (Leucine: $\delta^{15}N$ = -0.10 ± 0.24‰ and DORM 2: +14.95 ± 0.09‰) were used to normalize the results to the AIR scale based on international IAEA standards (N1, N2 and NO3). We measured a third internal standard (casein; $\delta^{15}N$ = -0.1 ± 0.15‰) to assess the normalization. Results are given in delta units (δ) in ‰ vs AIR. Overall analytical uncertainty (1σ) was calculated to be better than ± 0.2‰, based on the propagation of uncertainties of the normalization of internal reference materials and samples.

4.3 Spectral analysis

Cross-wavelet coherence and phase-relationship analyses were conducted using the Cross Wavelet and Wavelet Coherence toolbox in MatLab R2019a provided by A. Grinsted. For technical specifications of squared-wavelet coherence and phase-direction calculations, see ref. 44. Significance is reported at the 95% confidence level against red noise, which was determined via 300 Monte Carlo simulations. “In-phase” relationships describe those that represent positive correlations between variables and “antiphase” relationships describe negative correlations. To achieve equally-spaced $\delta^{15}N_{algal}$ values, five-year interpolations were calculated from the raw data and used for spectral analysis. In cases where $\delta^{15}N_{algal}$ data were analyzed against annually-

460 resolved records, data points corresponding to the $\delta^{15}N_{algal}$-interpolated year were used. Raw data
461 were used in analyses between two annually-resolved records.
462
463
464 **Author contributions**
465 BW and BT designed the study. WA collected the alga. EK subsampled the specimen and
466 developed the chronology. BT performed nitrogen isotope analysis. JMD conducted statistical
467 analyses, interpreted the data and wrote the text with input from all authors.
468
469 **Acknowledgements**
470 This study was funded by the *Seed Grant for Basic Research* #201611159215, University Research
471 Committee, awarded to BT and the NSF MGG-BIO #1459827 to BW. We are thankful to JF Hélie
472 (GEOTOP) for his assistance with nitrogen isotope measurements. All original data used in this
473 paper are made available in the online material.
474
475
476
477
478
479
480
481
482

References

1. F. Pithan, T. Mauritsen, Arctic amplification dominated by temperature feedbacks in contemporary climate models. *Nat. Geosci.* (2014), doi:10.1038/ngeo2071.
2. J. Halfar, W. H. Adey, A. Kronz, S. Hetzinger, E. Edinger, W. W. Fitzhugh, Arctic sea-ice decline archived by multicentury annual-resolution record from crustose coralline algal proxy. *Proc. Natl. Acad. Sci.* (2013), doi:10.1073/pnas.1313775110.
3. P. Chan, J. Halfar, W. Adey, S. Hetzinger, T. Zack, G. W. K. Moore, U. G. Wortmann, B. Williams, A. Hou, Multicentennial record of Labrador Sea primary productivity and sea-ice variability archived in coralline algal barium. *Nat. Commun.* (2017), doi:10.1038/ncomms15543.
4. T. Kuhlbrodt, A. Griesel, M. Montoya, A. Levermann, M. Hofmann, S. Rahmstorf, On the driving processes of the Atlantic meridional overturning circulation. *Rev. Geophys.* **45**, RG2001 (2007).
5. M. W. Buckley, J. Marshall, Observations, inferences, and mechanisms of the Atlantic Meridional Overturning Circulation: A review. *Rev. Geophys.* **54**, 5–63 (2016).
6. B. Thibodeau, C. Not, J. Zhu, A. Schmittner, D. Noone, C. Tabor, J. Zhang, Z. Liu, Last century warming over the Canadian Atlantic shelves linked to weak Atlantic Meridional Overturning Circulation. *Geophys. Res. Lett.* (2018), doi:10.1029/2018GL080083.
7. D. J. R. Thornalley, D. W. Oppo, P. Ortega, J. I. Robson, C. M. Brierley, R. Davis, I. R. Hall, P. Moffa-Sanchez, N. L. Rose, P. T. Spooner, I. Yashayaev, L. D. Keigwin, Anomalously weak Labrador Sea convection and Atlantic overturning during the past 150 years. *Nature*. **556**, 227–230 (2018).
8. L. Caesar, S. Rahmstorf, A. Robinson, G. Feulner, V. Saba, Observed fingerprint of a weakening Atlantic Ocean overturning circulation. *Nature*. **556**, 191–196 (2018).
9. M. S. Lozier, F. Li, S. Bacon, F. Bahr, A. S. Bower, S. A. Cunningham, M. F. De Jong, L. De Steur, B. DeYoung, J. Fischer, S. F. Gary, B. J. W. Greenan, N. P. Holliday, A. Houk, L. Houpert, M. E. Inall, W. E. Johns, H. L. Johnson, C. Johnson, J. Karstensen, G. Koman, I. A. Le Bras, X. Lin, N. Mackay, D. P. Marshall, H. Mercier, M. Oltmanns, R. S. Pickart, A. L. Ramsey, D. Rayner, F. Straneo, V. Thierry, D. J. Torres, R. G. Williams, C. Wilson, J. Yang, I. Yashayaev, J. Zhao, A sea change in our view of overturning in the subpolar North Atlantic. *Science* (2019), doi:10.1126/science.aau6592.
10. J. W. Loder, B. Petrie, G. Gawarkiewicz, in *The Sea*, A. Robinson, K. Brink, Eds. (Wiley, New York, 1998), pp. 105–133.
11. C. A. Stock, J. G. John, R. R. Rykaczewski, R. G. Asch, W. W. L. Cheung, J. P. Dunne, K. D. Friedland, V. W. Y. Lam, J. L. Sarmiento, R. A. Watson, Reconciling fisheries catch and ocean productivity. *Proc. Natl. Acad. Sci. U. S. A.* (2017), doi:10.1073/pnas.1610238114.
12. T. Takahashi, S. C. Sutherland, R. Wanninkhof, C. Sweeney, R. A. Feely, D. W. Chipman, B. Hales, G. Friederich, F. Chavez, C. Sabine, A. Watson, D. C. E. Bakker, U. Schuster, N. Metzl, H. Yoshikawa-Inoue, M. Ishii, T. Midorikawa, Y. Nojiri, A. Körtzinger, T. Steinhoff, M. Hoppema, J. Olafsson, T. S. Arnarson, B. Tilbrook, T. Johannessen, A. Olsen, R. Bellerby, C. S. Wong, B. Delille, N. R. Bates, H. J. W. de Baar, Climatological mean and decadal change in surface ocean pCO2, and net sea-air CO2 flux over the global oceans. *Deep. Res. Part II Top. Stud. Oceanogr.* (2009), doi:10.1016/j.dsr2.2008.12.009.

13. W. G. Harrison, K. Y. Børsheim, W. K. W. Li, G. L. Maillet, P. Pepin, E. Sakshaug, M. D. Skogen, P. A. Yeats, Phytoplankton production and growth regulation in the Subarctic North Atlantic: A comparative study of the Labrador Sea-Labrador/Newfoundland shelves and Barents/Norwegian/Greenland seas and shelves. *Prog. Oceanogr.* (2013), doi:10.1016/j.pocean.2013.05.003.
14. W. G. Harrison, W. K. W. Li, Phytoplankton growth and regulation in the Labrador Sea: Light and nutrient limitation. *J. Northwest Atl. Fish. Sci.* (2007), doi:10.2960/J.v39.m592.
15. S. A. Henson, J. P. Dunne, J. L. Sarmiento, Decadal variability in North Atlantic phytoplankton blooms. *J. Geophys. Res. Ocean.* (2009), doi:10.1029/2008JC005139.
16. K. F. Drinkwater, G. C. Harding, Effects of the hudson strait outflow on the biology of the Labrador Shelf. *Can. J. Fish. Aquat. Sci.* (2001), doi:10.1139/f00-210.
17. K. Rollings, "The hydrology of Labrador" (1997), (available at https://www.mae.gov.nl.ca/waterres/reports/hydrology_lab/index.html).
18. J. R. N. Lazier, D. G. Wright, Annual velocity variations in the Labrador Current. *J. Phys. Oceanogr.* (2002), doi:10.1175/1520-0485(1993)023<0659:avvitl>2.0.co;2.
19. M. A. Altabet, R. Francois, in *Carbon cycling in the glacial ocean: constraints on the ocean's role in global change* (1994).
20. A. Mariotti, J. C. Germon, P. Hubert, P. Kaiser, R. Letolle, A. Tardieux, P. Tardieux, Experimental determination of nitrogen kinetic isotope fractionation: Some principles; illustration for the denitrification and nitrification processes. *Plant Soil* (1981), doi:10.1007/BF02374138.
21. D. M. Sigman, F. Fripiat, Nitrogen Isotopes in the Ocean. *Encycl. Ocean Sci.* (2018).
22. P. K. Swart, S. Evans, T. Capo, M. A. Altabet, The fractionation of nitrogen and oxygen isotopes in macroalgae during the assimilation of nitrate. *Biogeosciences* (2014), doi:10.5194/bg-11-6147-2014.
23. H. Ren, D. M. Sigman, A. N. Meckler, B. Plessen, R. S. Robinson, Y. Rosenthal, G. H. Haug, Foraminiferal isotope evidence of reduced nitrogen fixation in the ice age Atlantic ocean. *Science* **323**, 244–248 (2009).
24. L. Muscatine, C. Goiran, L. Land, J. Jaubert, J. P. Cuif, D. Allemand, Stable isotopes ($\delta^{13}C$ and $\delta^{15}N$) of organic matrix from coral skeleton. *Proc. Natl. Acad. Sci. U. S. A.* (2005), doi:10.1073/pnas.0408921102.
25. D. P. Gillikin, A. Lorrain, A. Jolivet, Z. Kelemen, L. Chauvaud, S. Bouillon, High-resolution nitrogen stable isotope sclerochronology of bivalve shell carbonate-bound organics. *Geochim. Cosmochim. Acta* (2017), doi:10.1016/j.gca.2016.12.008.
26. P. Chan, J. Halfar, W. H. Adey, P. A. Lebednik, R. S. Steneck, C. J. D. Norley, D. W. Holdsworth, Recent density decline in wild-collected subarctic crustose coralline algae reveals climate change signature. *Geology*. **48** (2020).
27. G. W. K. Moore, J. Halfar, H. Majeed, W. Adey, A. Kronz, Amplification of the Atlantic Multidecadal Oscillation associated with the onset of the industrial-era warming. *Sci. Rep.* (2017), doi:10.1038/srep40861.
28. R. Schlitzer, Ocean Data View, https://odv.awi.de (2018).
29. H. E. Garcia, R. A. Locarnini, T. P. Boyer, J. I. Antonov, O. K. Baranova, M. M. Zweng, J. R. Reagan, D. R. Johnson, *World Ocean Atlas 2013, Volume 4: Dissolved Inorganic Nutrients (phosphate, nitrate, silicate)* (2013).
30. O. A. Sherwood, M. F. Lehmann, C. J. Schubert, D. B. Scott, M. D. McCarthy, Nutrient regime shift in the western North Atlantic indicated by compound-specific $\delta^{15}N$ of deep-

sea gorgonian corals. *Proc. Natl. Acad. Sci. U. S. A.* (2011), doi:10.1073/pnas.1004904108.

31. D. Marconi, M. A. Weigand, D. M. Sigman, Nitrate isotopic gradients in the North Atlantic Ocean and the nitrogen isotopic composition of sinking organic matter. *Deep Sea Res. Part I.* **145**, 109–124 (2019).
32. H. E. Garcia, T. P. Boyer, R. A. Locarnini, J. I. Antonov, A. V Mishonov, O. K. Baranova, M. M. Zweng, J. R. Reagan, D. R. Johnson, World Ocean Atlas 2013. Volume 3: dissolved oxygen, apparent oxygen utilization, and oxygen saturation. *NOAA Atlas NESDIS 75* (2013).
33. T. Dalsgaard, B. Thamdrup, L. Farías, N. P. Revsbech, Anammox and denitrification in the oxygen minimum zone of the eastern South Pacific. *Limnol. Oceanogr.* (2012), doi:10.4319/lo.2012.57.5.1331.
34. K. Harding, K. A. Turk-Kubo, R. E. Sipler, M. M. Mills, D. A. Bronk, J. P. Zehr, Symbiotic unicellular cyanobacteria fix nitrogen in the Arctic Ocean. *Proc. Natl. Acad. Sci. U. S. A.* (2018), doi:10.1073/pnas.1813658115.
35. M. Yamamoto-Kawai, E. Carmack, F. McLaughlin, Nitrogen balance and Arctic throughflow. *Nature* (2006), doi:10.1038/443043a.
36. D. Cote, K. Heggland, S. Roul, G. Robertson, D. A. Fifield, V. Wareham, E. B. Colbourne, G. Maillet, L. Pilgrim, "Canadian Science Advisory Secretariat (CSAS) Overview of the biophysical and ecological components of the Labrador Sea Frontier Area" (2019), (available at https://www.researchgate.net/publication/332144733_Canadian_Science_Advisory_Secretariat_CSAS_Overview_of_the_biophysical_and_ecological_components_of_the_Labrador_Sea_Frontier_Area).
37. M. E. Mann, B. A. Steinman, S. K. Miller, Absence of internal multidecadal and interdecadal oscillations in climate model simulations. *Nat. Commun.* **11** (2020).
38. J. W. Hurrell, Decadal trends in the North Atlantic oscillation: Regional temperatures and precipitation. *Science* (1995), doi:10.1126/science.269.5224.676.
39. B. Petrie, Does the North Atlantic Oscillation affect hydrographic properties on the Canadian Atlantic Continental Shelf? *Atmos. - Ocean* (2007), doi:10.3137/ao.450302.
40. M. E. Schlesinger, N. Ramankutty, An oscillation in the global climate system of period 65-70 years. *Nature* (1994), doi:10.1038/367723a0.
41. M. W. Miles, D. V. Divine, T. Furevik, E. Jansen, M. Moros, A. E. J. Ogilvie, A signal of persistent Atlantic multidecadal variability in Arctic sea ice. *Geophys. Res. Lett.* (2014), doi:10.1002/2013GL058084.
42. R. Zhang, R. Sutton, G. Danabasoglu, Y. O. Kwon, R. Marsh, S. G. Yeager, D. E. Amrhein, C. M. Little, A review of the role of the Atlantic Meridional Overturning Circulation in Atlantic Multidecadal Variability and associated climate impacts. *Rev. Geophys.* (2019), doi:10.1029/2019RG000644.
43. J. R. Knight, R. J. Allan, C. K. Folland, M. Vellinga, M. E. Mann, A signature of persistent natural thermohaline circulation cycles in observed climate. *Geophys. Res. Lett.* (2005), doi:10.1029/2005GL024233.
44. A. Grinsted, J. C. Moore, S. Jevrejeva, Application of the cross wavelet transform and wavelet coherence to geophysical time series. *Nonlinear Process. Geophys.* (2004), doi:10.5194/npg-11-561-2004.
45. V. Trouet, J. Esper, N. E. Graham, A. Baker, J. D. Scourse, D. C. Frank, Persistent

positive North Atlantic Oscillation mode dominated the medieval climate anomaly. *Science* (2009), doi:10.1126/science.1166349.

46. S. T. Gray, L. J. Graumlich, J. L. Betancourt, G. T. Pederson, A tree-ring based reconstruction of the Atlantic Multidecadal Oscillation since 1567 A.D. *Geophys. Res. Lett.* (2004), doi:10.1029/2004GL019932.
47. P. Moffa-Sánchez, I. R. Hall, S. Barker, D. J. R. Thornalley, I. Yashayaev, Surface changes in the eastern Labrador Sea around the onset of the Little Ice Age. *Paleoceanography* (2014), doi:10.1002/2013PA002523.
48. S. Rahmstorf, J. E. Box, G. Feulner, M. E. Mann, A. Robinson, S. Rutherford, E. J. Schaffernicht, Exceptional twentieth-century slowdown in Atlantic Ocean overturning circulation. *Nat. Clim. Chang.* **5**, 475–480 (2015).
49. M. Claret, E. D. Galbraith, J. B. Palter, D. Bianchi, K. Fennel, D. Gilbert, J. P. Dunne, Rapid coastal deoxygenation due to ocean circulation shift in the northwest Atlantic. *Nat. Clim. Chang.* (2018), doi:10.1038/s41558-018-0263-1.
50. M. B. Osman, S. B. Das, L. D. Trusel, M. J. Evans, H. Fischer, M. M. Grieman, S. Kipfstuhl, J. R. McConnell, E. S. Saltzman, Industrial-era decline in subarctic Atlantic productivity. *Nature* (2019), doi:10.1038/s41586-019-1181-8.
51. A. Schmittner, Decline of the marine ecosystem caused by a reduction in the Atlantic overturning circulation. *Nature* (2005), doi:10.1038/nature03476.
52. E. Ehrnsten, B. Bauer, B. G. Gustafsson, Combined effects of environmental drivers on marine trophic groups – a systematic model comparison. *Front. Mar. Sci.* (2019), doi:10.3389/fmars.2019.00492.

667 **Supplementary Material**

Prediction	Predictors	Coefficient	p-Value	Adj. R^2
Salinity	∇S	0.502	1.94E-08	0.56
	T	0.234	2.17E-12	
	∇T	-0.113	0.001	
Temperature Proxy	∇Tprox	0.489	2.83E-13	0.57
	T	0.283	3.85E-07	
	∇T	-0.106	0.066	

668
669 **Table S1: Regression results.** (top) Observational salinity anomalies (S) predicted from
670 observational temperature anomalies (T) from 1929 – 2009 (*36*), and (bottom) temperature proxy
671 anomalies (Tprox) (*27*) predicted from observational temperature anomalies from 1929 – 2010**.**
672 To account for AR(1) autocorrelation, first-difference terms were included in both models,
673 represented by inverted triangles in the table. Both analyses were performed in RStudio version
674 1.2.1335.
675

676

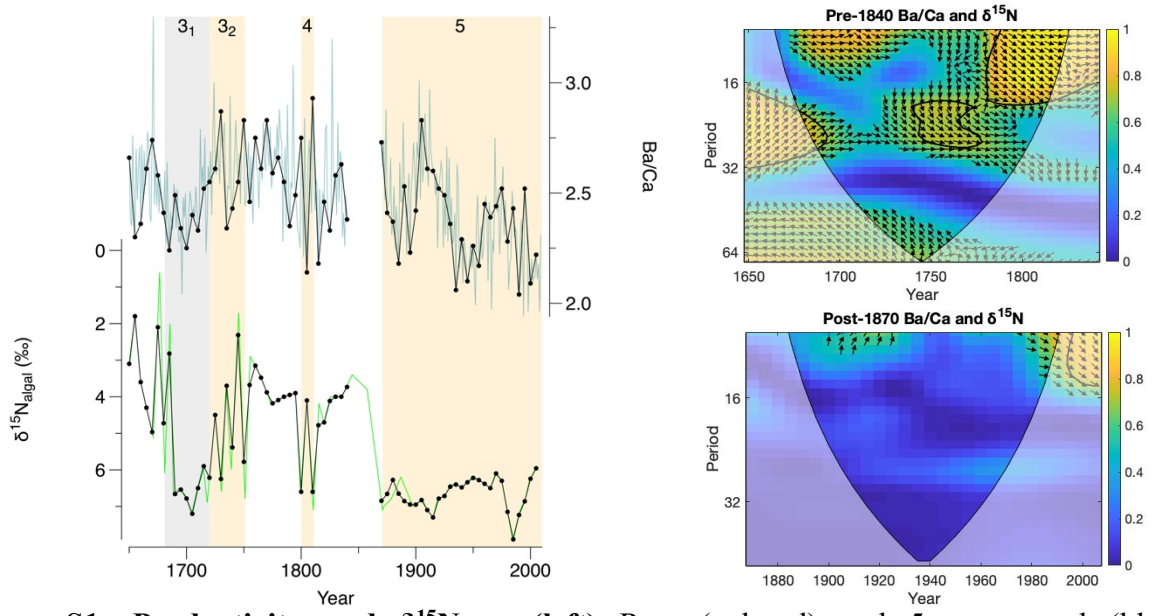

677
678 **Figure S1: Productivity and $\delta^{15}N_{algal}$. (left)** Raw (colored) and 5-year-spaced (black)
679 productivity reconstructed from Ba/Ca (*3*) plotted with raw (colored) and 5-year-spaced (black)
680 $\delta^{15}N_{algal}$ values. Phase 3_1 is represented by the grey-shaded region and other phases are represented
681 by tan-shaded regions; **(right)** cross-wavelet coherence and phase relationships between 5-year-
682 spaced Ba/Ca and $\delta^{15}N_{algal}$ data during the 1660 – 1840 and 1870 – 2005 intervals. For a full
683 description of the wavelet plots, see the legend of Figure 4.
684